



UDC 621.923

THEORETICAL AND EXPERIMENTAL STUDY OF DOUBLE-SIDED GRINDING PROCESS OF ROUND FACE ENDS BY ORIENTATED WHEELS WITH CALIBRATING SECTIONS

Dmytro Kalchenko

Chernihiv National University of Technology, Chernihiv, Ukraine

Summary. The developed 3D model first determines the overall machining efficiency Q_s of two round face ends processing, for example, cross-pieces, pushers, depending on the coordinate θb along the entire length of the contact line L . It is equal to the sum of the grinding performance of all parts located in the processing area on each of the wheels edges. For the first time a general methodology of theoretical and experimental research of specific and general: productivity, power and cutting forces on the left and right face ends of the part, the sum of which is equal to the total productivity on both ends, has been developed. The method of determining the connection of the current angular coordinate of the axis of the part with the required processing time is developed. While the part machining is carried out on the calibration section, the next part is not fed to the processing area, which eliminates the influence of the transition process on the accuracy of shape forming, and the efficiency improving is ensured by the fact that the next part enters the processing area immediately after the release of the part from the calibrating section.

Key words: grinding, face ends of the parts, oriented grinding wheels, grinding capacity.

Received 15.01.2018

Problem setting. In machine-tool technology, mechanical engineering, automobile and bearing industry the parts with high-precision round face end surfaces are widely used. That is bearing rollers, cross-pieces of cardan shafts, pushers and other parts. The final accuracy of them is provided by finish operations. In the conditions of further development of market relations, the development of new methods of grinding and theoretical and experimental researches, which substantiate their efficiency, and provide increased productivity and accuracy of machining of parts with round face end surfaces is the actual problem.

Actual scientific research and issues analysis. On the two-sided end-grinding machines of the company Saturn (Germany) [1] the machining of parts round face ends with a circular feed to the processing area is processed. Abrasive wheels without calibrating sections are used, that requires multi pass machining to obtain the required accuracy and this reduces the productivity of grinding.

The high efficiency method is developed [2] and theoretically researched [3] regarding the one-pass double-sided grinding of round face ends of parts using abrasive wheels with calibrating sections, which provides an increase in the accuracy of shape forming as well as the quality of the machined surface and productivity due to one-pass grinding.

The paper [4] investigates the influence of the length of the calibrating section of the wheel, the machining allowance, the diameter of the face ends of the parts, the diameter of the wheels and their orientation on the geometric accuracy that is the flatness deviation as well as deviation from perpendicularity and the parallelism of the face ends. The influence of parts rotation on the calibrating sections of wheels on the geometric error of the shape forming of the face ends is also researched. Its reducing, when the parts are rotated, is also shown. But it is not taken into account the gap between the diameter of the part and the hole in the feeding drum,

where the part is based. That reduces the accuracy depending on the length of the part and its diameter as well as on the size of the gap and the values of the tangential and normal components of the cutting forces during machining. So the influence of the rotation of the part on the accuracy of shape forming requires further research.

In the papers [3,4] the productivity of the double-sided grinding of round face ends is investigated. However, productivity is considered only for one face end of the part and the productivity of grinding for the second face end, grinding power, cutting forces, total productivity, wear of wheels were not considered.

Increasing the productivity and accuracy of machining requires theoretical and experimental study of the grinding processes on each face end as well as their influence on the overall productivity and accuracy.

The research objective. The research objective is to develop the 3D model of the machining efficiency of each face end of the part and the total overall productivity as well as formulation of the general methodology of theoretical and experimental research of specific, under machining coordinate at each face end and general values of: grinding performance, power and cutting forces which increase the efficiency of evaluation of new ways of grinding face ends.

For two-sided grinding of face ends there are two simultaneous processes with different coordinates of machining on each face end in regard to the removable allowances, cutting forces, actual productivity, wheels wearing, grinding capacities, heating temperatures of face ends, flexibility of technological systems from wheels to the face ends. It significantly affects overall productivity on each face end of the wheels and on the overall efficiency and the machining accuracy of the two face ends of part. To evaluate the effectiveness of new ways of face ends grinding we need to develop a 3D model of machining efficiency of each face end and of the total productivity, based on which the new high effective methods of face ends grinding will be created.

The statement of basic materials. Fig. 1 shows a diagram of the process of two-sided grinding of round face ends, for example: cross-pieces of cardan shafts, pushers, bearing rollers, using grinding wheels 1, 2 with calibrating sections 3, 4. The parts 5 are fixed with a gap in the product feed drum 6, in the holes 8 (Fig. 1, A -A). The grinding wheels 1, 2 together with the wheel heads of the two-sided end-grinding machine are turned to the angles ψ in the vertical and φ in the horizontal planes. The orientation angles of the grinding wheels are selected depending on the size of the allowance, which is removed from the workpiece. The dressing of calibration sections 3, 4 is carried out by a diamond pencil 7, which is located within a radius $R_a = R_b$. When the parts 5 are fed into the machining area along the guides 11 with the required clearance $\Delta\delta$, the parts 5 are shifted axially by the value $\Delta\delta$ (Fig. 1, B), which increases the removable allowance on one face end and reduces it on the second, which results in different productivity, cutting forces, wheels wear.

The torque M , which rotates parts 5 during machining (Fig. 1), is determined by the formula:

$$M = 2(R_{\max} - R_{\min}) \cdot P_z \quad , \quad (1)$$

where P_z is the value of the cutting force at the maximum R_{\max} and the minimum R_{\min} of the grinding wheel radius 1 contact with the parts 5 with diameter d .

The analysis of formula (1) shows that when the part enters the machining area and touches the diameter of the wheel, which is equal to $R_v - L_k$ (Fig. 1), $L_k = d$, in this case $R_{min} = 0$, and the wheel, due to the cutting forces P_z , begins to rotate the part counter clockwise at a speed approaching to the speed of the grinding wheel, with a decrease in the coefficient of slipping motion of the part. In this case there is a transition process in which there is no time to make the allowance and the intense wearing of the wheel begins. In the process of moving of the part 5 with the feed drum 6, the speed of the rotation of the part gradually decreases and when the contact includes the entire face end and the radiuses R_{max}, R_{min} touch the part the transition process is over. So there is a torque (1) that rotates the part clockwise (Fig. 1). At the output of the part from the roughing area to the calibrating section the cuttings force P_z decrease, as the contact occurs along the line, and with a small depth of grinding, and when the face end of the part outside the outer diameter of the wheel R_v, R_{min} , gradually decreases to 0. In this case the direction of rotation varies and the part begins to rotate counter clockwise. The transient process begins due to increase motion of the part by the maximum diameter of the wheel $R_{max} = R_v$ at the end of the calibrating section with low intensity (1). The experimental study of the rotation of the part by the cutting forces for double-sided grinding was first performed by the author [5], where the speed of the piston pin was measured by a digital laser contactless tachometer HS2234.

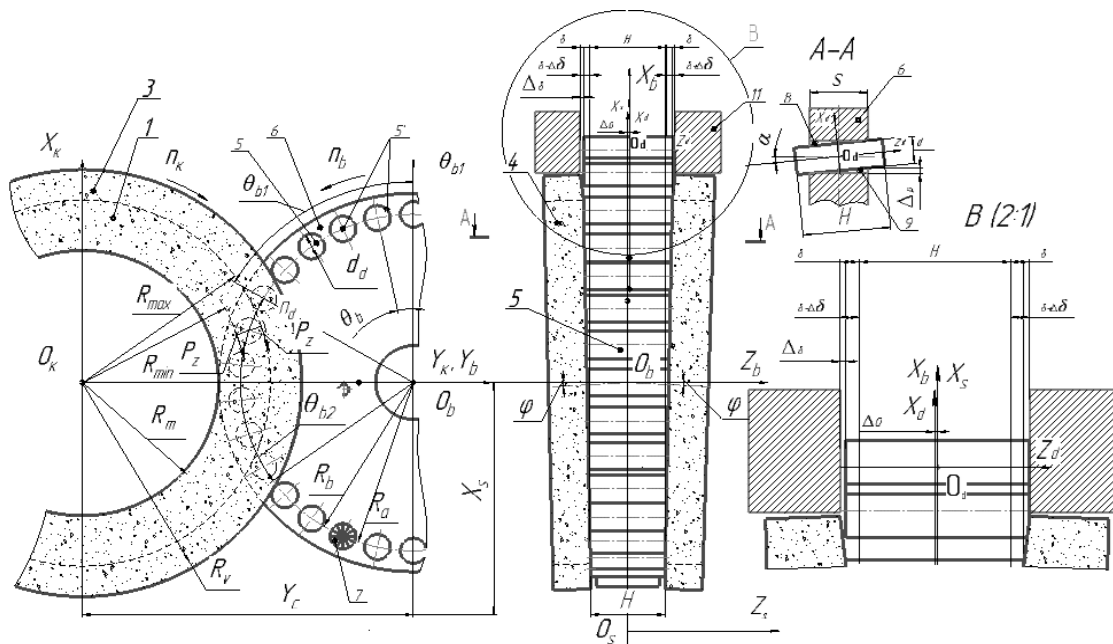


Figure 1. Scheme for machining of bearing rollers 5 and pushers 5', which rotate in the holes of the feeding drum

When machining the face ends of rollers of bearings 5 (Fig. 1) which are rotated during the grinding, the locating is carried out in the holes 8 of the feed drum 6 with a gap Δp , which results in the non perpendicularity of the face ends to the axis of the part due to their turn at the angle α , which is equal to

$$\text{tg } \alpha = \frac{\Delta p}{S}, \quad (2)$$

where S is the height (Fig. 1, A-A) of the feeding drum 6.

Therefore, when machining the high-precision parts it is customary to locate them without gaps as shown in Figure 2, which occurs when loading parts 5 (Fig. 2) in location prism 9, where they are pressed by forces P , which lie in planes passing through the parts 5 axis and axis of the feeding drum 6. The forces P are provided by the chain mechanism 10, where the speed of the chain V_l and the parts 5 is equal on the clamping area. This is ensured by the transmission ratio of the drum drive 6 and the driving star 12.

When grinding pushers 5' of different diameters, they are located in the holes 8 (Fig. 3a, A-A) of the drum 6 with a gap Δr , from which there is non perpendicularity of the face ends to the axis of the part due to their turn at the angle α , which is calculated by the formula (2).

The torque M , which rotates the pusher 5' (Fig. 1), (Fig. 3a) during machining, is determined by the formula

$$M = (R_{\max D} - R_{\min D}) \cdot P_{zD} - (P_{nD} - P_{nd}) \cdot f \cdot R_t + (R_{\max d} - R_{\min d}) \cdot P_{zd}, \quad (3)$$

where P_{zD} is the value of the tangential cutting force at the maximum $R_{\max D}$ and minimum $R_{\min D}$ touch radiuses of the grinding wheel 2 and the part 5' of diameter D ; P_{nD} , P_{nd} are the normal components of the cutting force on the larger and smaller face ends; f is a coefficient of friction on the face end of the drum hub; R_t – radius of friction of the pusher on the drum hub 6; P_{zd} – the value of the tangential cutting force at the maximum $R_{\max d}$ and minimum $R_{\min d}$ touch radiuses of the grinding wheel 1 and the part 5' of diameter d .

The analysis of the formula (3) shows that the larger diameter D enters first the machining area and touches the diameter of the wheel 1, which is equal to $R_v - L_k$ (Fig. 3a), $L_k = D$ and wheel 1, due to the cutting forces P_{zD} , begins to rotate the part counter clockwise at a speed, which is approaching the speed of the grinding wheel, there is a transient process. When the feeding drum is moved to the value equal to $D/2 - d/2$, the machining of the face end of the smaller diameter begins, on which the torque and the normal component P_{nd} (3) appear. In the process of moving the part by the drum, when the face end of the part D comes in contact, the radiuses R_{\max} , R_{\min} , touch the part and the transition process is over (Fig.1), (Fig. 3a, the lower pusher). In this case a torque M (3) appears, and at the exit of the larger face end of the part diameter outside the outer wheel diameter $R_v = R_{\max}$, and R_{\min} gradually decreases to 0. In this case the direction of rotation changes, there is a transient process due to the increase motion of the part with a larger wheel diameter R_v .

As $P_n \leq 3 P_z$, the coefficient of friction $f \leq 0.15-0.2$, $R_t \leq D/2$, the torque calculated by the formula (3) for the maximum values, P_n , f , R_t is greater than the friction time, so the part will always be rotated.

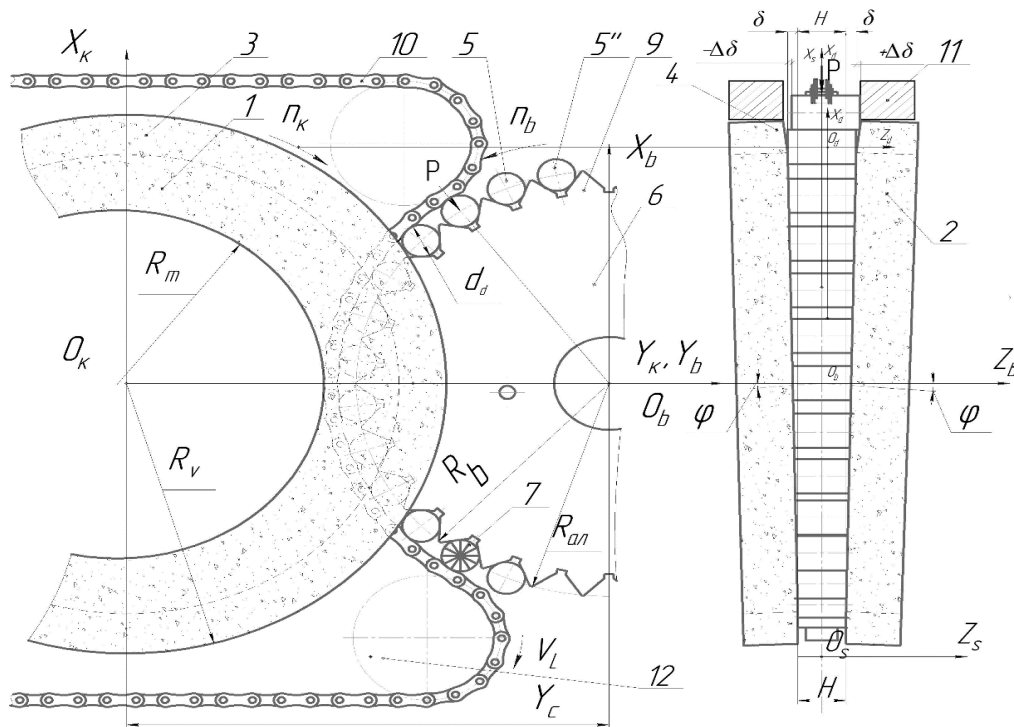


Figure 2. Scheme for machining bearing rollers, pushrods and crosses that do not rotate in the prism of the feeding drum

When grinding, the maximum non-perpendicularity, calculated by the formula (2), arises on a larger diameter D (Fig. 3, A-A) and if it exceeds permissible, then the locating is executed in prisms 9 (Fig. 2) for a zero black-lash scheme. The machining is carried out according to the new developed method of face ends grinding with the rotation of each next pusher at 180° , which aligns on the right p and the left l ends: the total normal cutting forces P_{nl}, P_{np} , the efficiencies of machining Q_l and Q_r (4), wheels wearings I_{inl}, I_{inr} , total flexibility of Y_{il}, Y_{ir} technological systems and also increases the productivity and precision of grinding.

When grinding crosses 5" (Fig. 3b) with an axial fixation in the prisms 9 of the drum 6 (Fig. 3b, type B) there is an location error Δo along the axis of the workpiece, which increases the asymmetry of the face ends. In order to improve the accuracy of machining, it is necessary to reduce the allowance errors, and the error of the base Δo .

Maximum productivity, which provides the necessary accuracy and quality, is an integral indicator of the grinding process of different surfaces. The developed 3D model for the first time determines the overall productivity Q_s of the machining of two round face ends, for example: crosses of cardan shafts, pushers, bearing rollers and other parts depending on the coordinate θ_b throughout the length of the contact line L . It is equal to:

$$Q_s = Q_l + Q_p \quad (4)$$

where Q_l and Q_p are the machining productivity of the left and right face ends of the parts.

The left face end in the coordinate system of the part (Fig. 1,2) has the coordinate $-Z_d = -H/2$, and the right $Z_d = H/2$, where H is the length of the part.

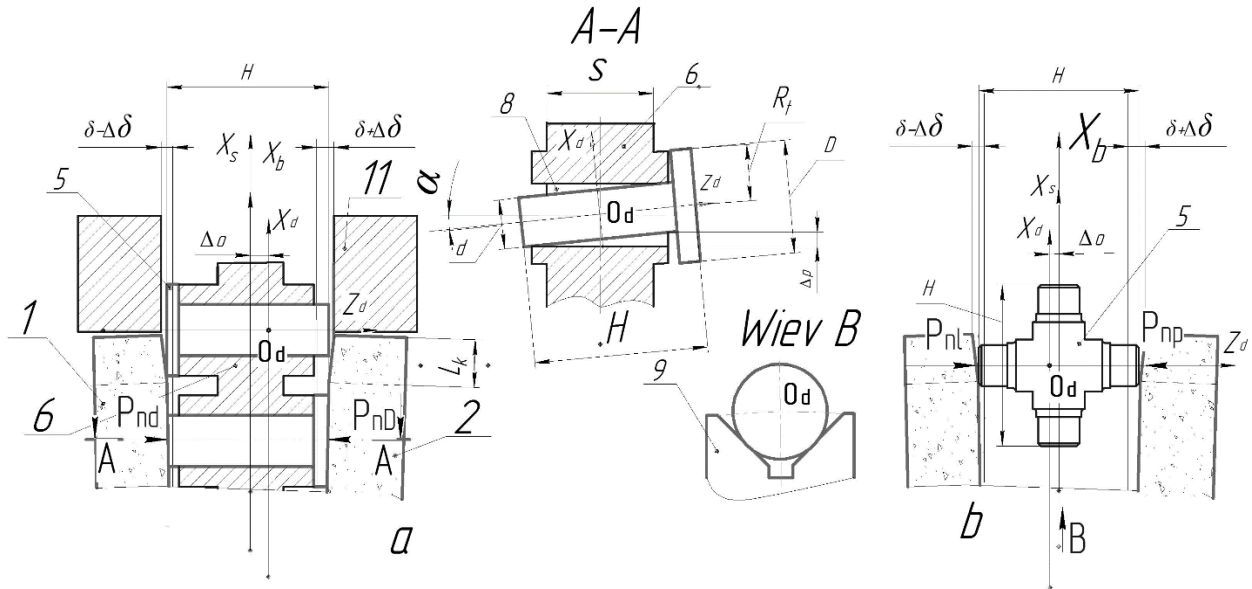


Figure 3. Circulation scheme of round face ends with axial fixation of parts in the prism: a – grinding pusher with different diameters of the ends and b – polishing cross-sections with axial fixation in the prism of the feeding drum

$$\begin{aligned}
 Q_s = & \sum_{n=1}^m \left(\int_{i_1^l}^{i_2^l} \left(\int_{\theta_{1kil}}^{\theta_{2kil}} \vec{V}_{inl} \cdot \vec{n}_{inl} \cdot (R_{il} - I_{inl} \cdot \sin \alpha_{inl} - Y_{inl} - \Delta\delta - \Delta\sigma) \cdot \right. \right. \\
 & \cdot [1 - \exp(-\frac{\sum b(t, \theta)}{b_0})] \cdot d\theta_{kil} \cdot \sqrt{(\frac{dR_{inl}}{di})^2 + (\frac{dz_{inl}}{di})^2} \cdot di \cdot dTn) + \\
 & + \left(\int_{i_1^p}^{i_2^p} \left(\int_{\theta_{1kip}}^{\theta_{2kip}} \vec{V}_{inp} \cdot \vec{n}_{inp} \cdot (R_{ip} - I_{inp} \cdot \sin \alpha_{inp} - Y_{inp} + \Delta\delta + \Delta\sigma) \right. \right. \\
 & \left. \left. [1 - \exp(-\frac{\sum b(t, \theta)}{b_0})] \cdot d\theta_{kip} \cdot \sqrt{(\frac{dR_{inp}}{di})^2 + (\frac{dz_{inp}}{di})^2} \cdot di \cdot dTn) \right), \right. \tag{5}
 \end{aligned}$$

where m is the number of simultaneously machined parts 5 (Fig. 1,2);

T_n – time of contact of n -th part 5 with the wheels 1,2;

$i_{1l}, i_{2l}, i_{1p}, i_{2p}$ – the boundary values of the parameter i and the axial section of the wheels 1,2 in the contact area (Fig. 1,2); and [2, p.92];

$\theta_{2kil}, \theta_{1kil}, \theta_{2kip}, \theta_{1kip}$ – angular coordinates of contact spot on radiuses $R_{il} - I_{inl} \cdot \sin \alpha_{inl}, R_{ip} - I_{inp} \cdot \sin \alpha_{inp}$ (Fig. 3); and [2, p.92];

$1 - \exp(-\frac{\sum b(t, \theta)}{b_0})$ – the probability of removal of the material of the workpiece [2, p.92];

$I_{inl}(\theta_b), I_{inp}(\theta_b)$ – wear of grinding wheels, which arises from a temporary resistance, which depends on the temperature of the heating of the part [5];

$\alpha_{inl}, \alpha_{inp}$ – angles of inclination in the i -th point of the profile, defining the direction of wear (Fig. 3); and [2, p.92];

Y_{inl}, Y_{inp} – total flexibility of technological systems (Fig. 3); and [5];

$\Delta\delta$ – displacement δ (Fig. 1,2);

Δo – axial displacement of the beginning of the O_d coordinate of the part 5 from the symmetry plane of the drum 6 (Fig. 1,2,3) which passes through the drum axis X_b, X_s of the frame.

The number m of parts, which are simultaneously machined on the machine, are determined from the expression:

$$m = \frac{L}{d} + \epsilon_p, \quad (6)$$

where $L = R_b \cdot \theta_{b2}$ is the length of the contact arc on the radius R_b , of the feeding drum 6 of the parts 5 with wheels 1,2 within the angle θ_{b2} ;

θ_{b1}, θ_{b2} are the angles of the part position at the beginning of the machining and at the points n ;

d – the outer diameter of the part 5;

b_p - distance between the parts on the radius R_b of the feeding drum.

In determining the number of crosses of cardan shafts 5" that are simultaneously machined, in the formula (6), instead of the outer diameter d of the part, the length H of the cross-section is placed (Fig. 3, b).

In determining the productivity in equation (5), integration is carried out in time T_n , and the basic angle coordinate θ_b of the part axis that determines the depth of cutting, the cutting forces, the wheels wearing, the volume of the removed material, is given in degrees. Therefore, for integrating in time the coordinate θ_b relation with time T_n is needed. The developed formula (7) defines such a relation

$$\frac{\theta_b}{1^\circ / t} = T_n, \quad (7)$$

where: θ_b – current coordinate angle of the part axis within the angle θ_{b2} of the drum; $1^\circ / t = \omega$ – angular velocity, which provides the machining time T_n ; t is the passage time of the part 1° within the angle θ_{b2} .

In the theoretical calculation of the technological system flexibility, it is necessary to determine not only the components of the tangential force of cutting $P_{z\theta b}$ along the machining coordinate θ_b , but also the normal components $P_{n\theta b}$, calculated from the formulas given in [6]. The power $N_{\theta b}$ is calculated by the formula

$$N_{\theta b} = P_{z\theta b} \cdot V_{\theta b}, \quad (8)$$

where $V_{\theta b}$ is a grinding speed according to the processing coordinate θ_b .

In theoretical and experimental studies, the total specific cutting forces $P_{z\theta b}$ and the power $N_{\theta b}$ at the coordinate θ_b of machining the values $\sum P_{z\theta b}, \sum N_{\theta b}$ are summed at the entrance of each subsequent detail until all the parts fill the machining zone θ_{b2} , and then, with the continuous supply of parts to the machining area, $\sum P_{z\theta b}, \sum N_{\theta b}$ change at the input of each the next part on the difference in the P_z cutting forces.

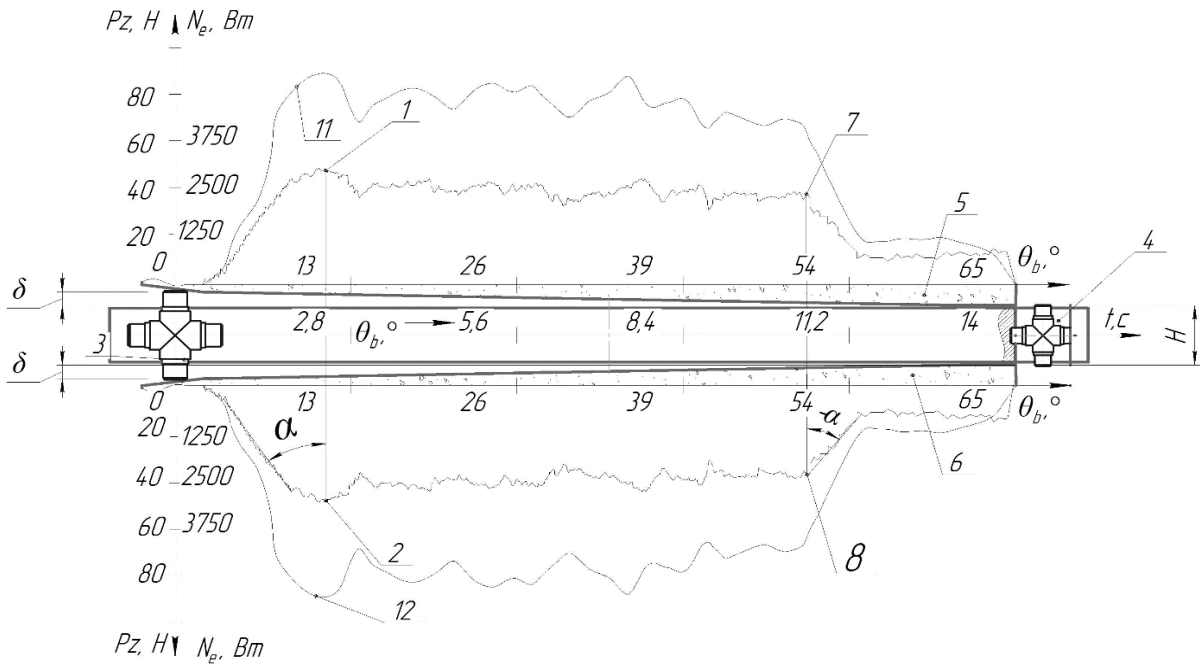


Figure 4. Active power and cutting forces by coordinate θ_b of machining on two face ends of one cross-piece

On the basis of the proposed general methodology, for the first time, an experimental study of total active power, and grinding forces at the coordinate θ_b of machining one cross-piece 3 (Fig. 4) was performed.

Experimental powers 1, 2 when two face ends grinding of the cross are depicted on fig. 4. When machining the face ends of the stud $\varnothing 16.3$ of the cross-piece 3, the power gradually increases to the time moment (points 1 and 2), when the cross-piece completely enters the zone of roughing, where the grinding is carried out by the flat face ends of the wheels on which the vectors of unit normal n_{in} n_{il} (5) are constant. So the value of the removed allowance is constant to the calibrating sections of the wheels (Fig. 4, point 7.8), after which the round face ends come out of the roughing zone and the power decreases according to the same regulation (the inclination angle of the tangent line – α), as it increased at the beginning of machining to the points 1,2 (inclination angle of the tangent line is α). Then the face ends of the pilot are machined with calibrating sections 5, 6 of the wheels. The finish grinding is carried out (where V_n $n_{in} = 0$). The process of shape forming is performed without the removal of the allowance, and the exit of the cross-piece 4 from the machining zone is taken place.

On the basis of capacities $N_{\theta b}$ (fig. 4), the cutting forces $P_{z\theta b}$ are calculated by the formula

$$P_{z\theta b} = \frac{N_{\theta b}}{V_{\theta b}}, \tag{9}$$

On Fig. 4 we also show the total cutting forces P_z 11,12 when machining the two face ends of the pin $\varnothing 16.3$ of the cross-piece 3, which are calculated by the formula (9). At the entrance, the forces increase, then they are constant at the flat face ends of the wheels and decrease with the exit from the roughing zone.

On Fig. 5, the specific processing powers at coordinates θ_b are shown in columns 1', 2', 3', 4', and the total power 3, which is equal to the sum of specific capacities on the two face ends, are shown with the continuous supply of crosses to the machining area. When moving the cross-piece from position V into the position I the specific power is indicated by the columns 1', 2', 3', 4', and the total power is given by the sum of the columns 1'-4'. The maximum value of the total power will be at the point where the calibrating section starts. Then it begins to decrease by the magnitude ΔN_{Σ} – the cross-piece is being machined by a calibrating area. At the exit of the cross-piece from the calibration section, the following raw cross is fed into position V.

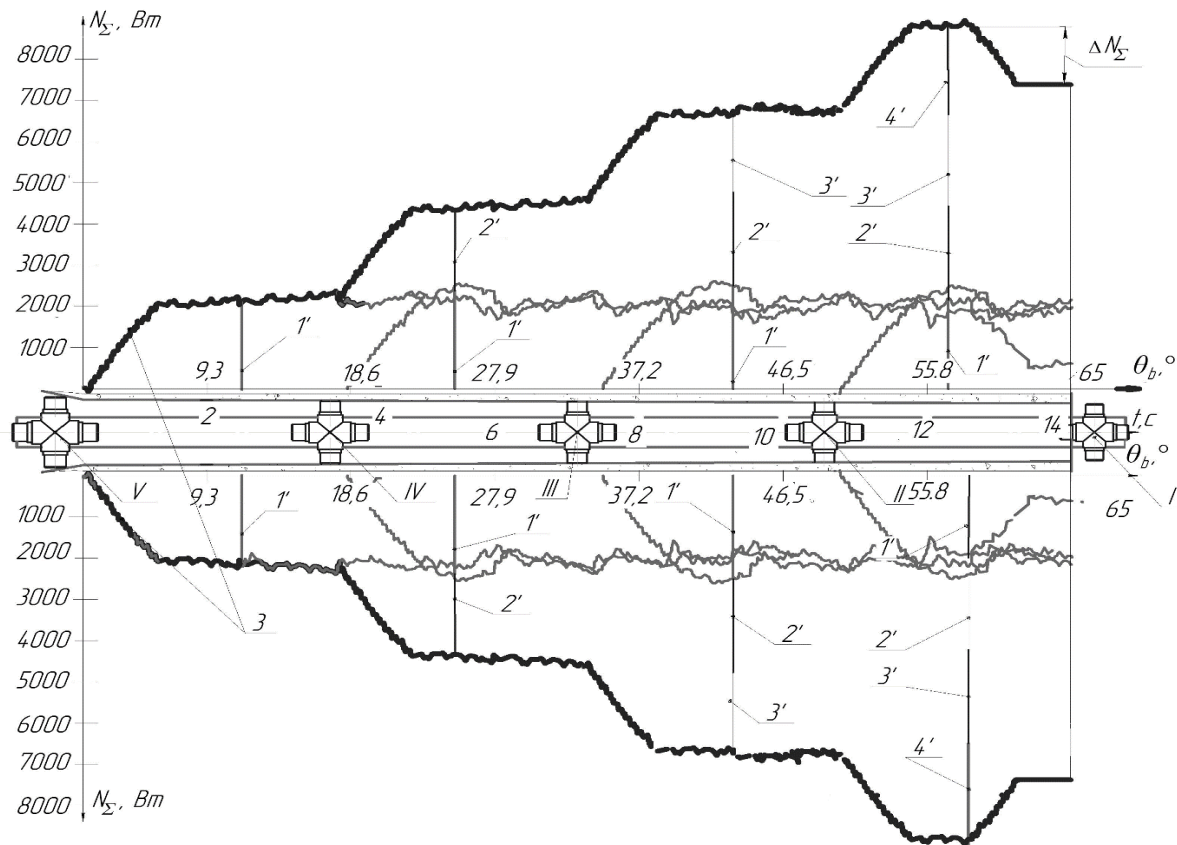


Figure 5. Specific and total active power, on two face ends, with continuous supply of crosses to the machining area

Also, the experimental research was carried out regarding the powers and cutting forces of the pusher according to the coordinate θ_b of machining with different face ends diameters. Grinding is carried out in a new developed way.

Fig. 6 shows a graph of power and cutting forces against the coordinate θ_b of machining on two face ends of one pusher. The power is indicated by curves 1 and 2, and the cutting forces are curves 5 and 6.

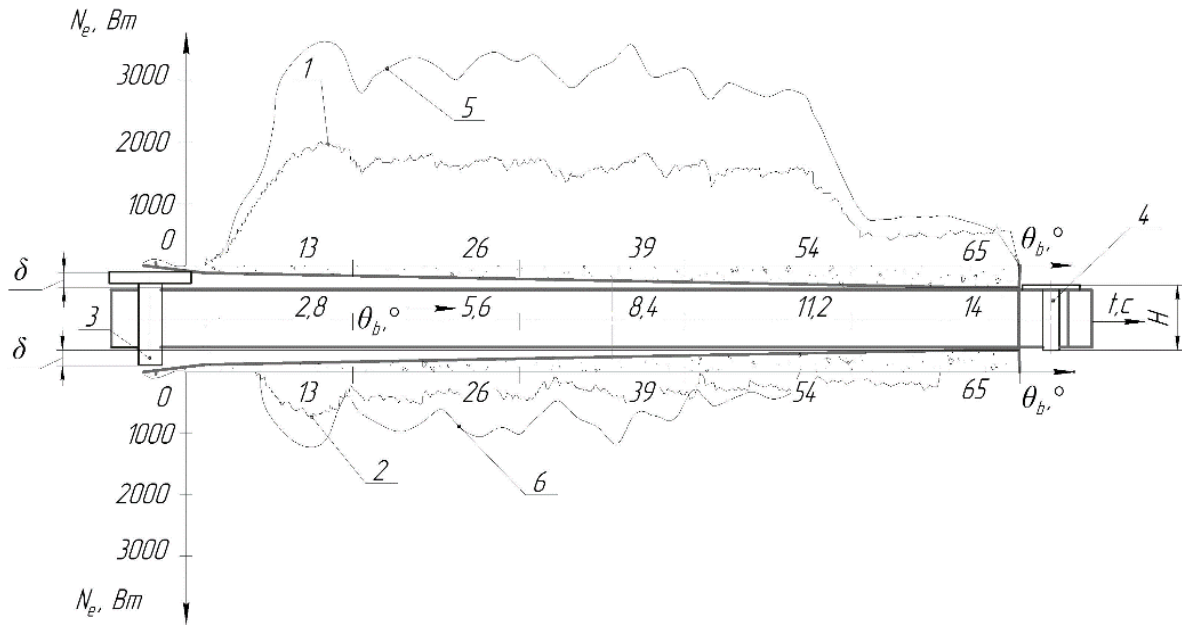


Figure 6. Active power by coordinate θ_b of machining on two face ends of one pusher

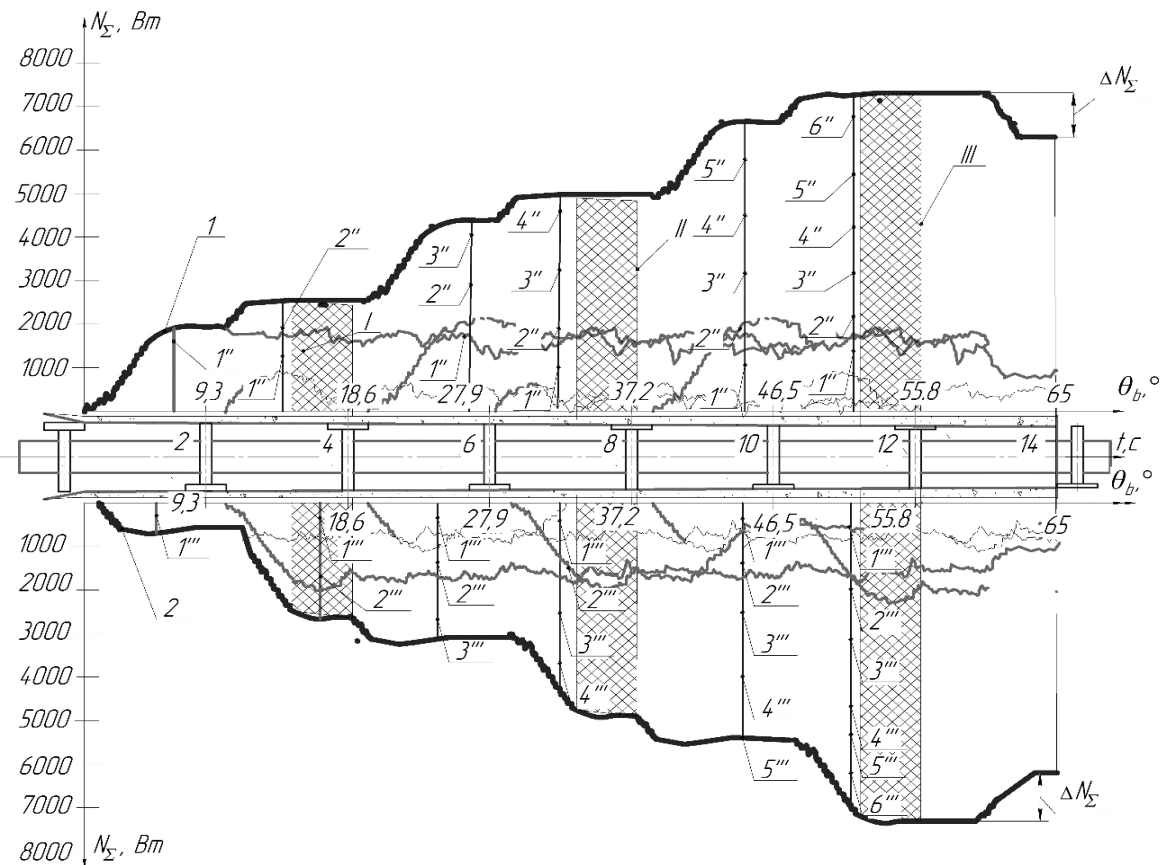


Figure 7. Specific and total active power on two face ends, with continuous supply of pushers to the machining area

On Fig. 7, the specific powers according the machining coordinate θ_b are shown in columns 1", 2", 3", 4", 5", 6" as well as the total power $1,2$ which is equal to the sum of specific capacities on two face ends, with continuous supply of pushers to the machining area. When the pushers are fed to the machining area, the specific powers are indicated by the columns 1", 2", 3", 4", 5", 6" and the total power is given by the sum of the columns 1" – 6". The maximum value of the total the power will be at the point where the calibrating area begins. Then it starts to decrease by magnitude ΔN_Σ and the pusher is machined with a calibrating section. When the pusher is released from the calibrating area, the following rough pusher is fed into the processing zone.

As can be seen from the figure, the first pusher enters by its larger face end. This leads to an increase in power by a value of 1", the smaller diameter begins machining with a delay on the difference in radii, and the increase in power takes place on the value of 1". Subsequently, the total power in the machining of pusher is fundamentally different from that of processing cross-pieces, as the next pusher enters the processing area turned into an angle of 180° . Then the values 1" and 1'" are changed by places. The zone I appears, which will be equal to the upper and lower parts of the graph. With continuous machining the zone I will repeat it – will be zones II and III accordingly.

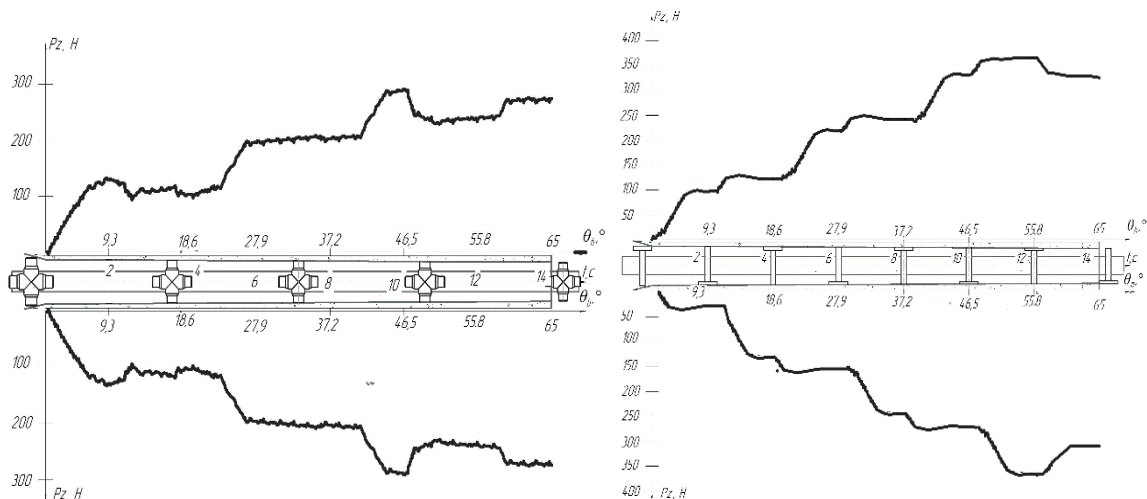


Figure 8. Total cutting force P_z according to the coordinate θ_b of machining on two face ends with continuous supply of pushers to the machining area

On Fig. 8 the current total force P_z is shown with continuous supply of cross-pieces (Fig. 8a) and pushers (Fig. 8b) to the processing area according to the machining coordinate θ_b . The force P_z is calculated by the formula (9) in which the values of maximum power are substituted for both cross-pieces and pushers.

All experimental studies shown in (Figs. 4-8) were carried out at a constant angular velocity of the drum $\omega = 4.61^0/c$, and the angle $\theta_{b2} = 65^0$ which correspond to the machining area, for parts that were not rotated during machining.

Conclusions. The developed 3D model (5) for the first time determines the overall productivity Q_s for machining of two round face ends, for example: cross-pieces of cardan shafts, pushers, bearing rollers and other parts, depending on the machining coordinate θ_b throughout the length of the contact line L . It is equal to the sum of the productivities of all parts that are in the machining area on each face end of the wheel. It has been proved for the first time that when two-sided grinding of the face ends there are simultaneously two processes with different coordinates θ_b of machining on each face end of the wheels with regard to the cutting

forces, removable allowances, wheels wearing, heating temperatures of face ends, flexibilities of technological systems from wheels to the face ends, instantaneous productivities, grinding capacities. Such factors essentially affect the overall performance on each face end of the wheels and the total productivity and machining accuracy of the two face ends of the parts.

Regarding the continuous supply of parts to the machining area for the first time a general methodology for determining the total power and cutting forces on each of the face ends was developed. It begins with the calculation of the power and cutting forces for one part, and then the power and cutting forces in the process of machining of the following parts are summed by the processing coordinate θ_b , after filling the parts of the processing zone (Fig. 1) on each of the face ends of the wheel. The total productivity, the cutting forces and the power in the continuous supply of parts to the machining area have the maximum values, but when the part runs to the calibrating area these values reduce by the difference in capacities at the rough and calibrating sections (Fig. 5, 7).

While the part machining is carried out on the calibrating section, the next part is not fed to the processing area. That eliminates the transition process influence on the accuracy of shape forming, and the productivity is ensured due to the fact that the next part enters the machining area immediately after the release of the previous part from the calibrating area (Fig. 5, 7).

The method of determining the relation of the current angular coordinate θ_b with the machining time T_n is developed.

A new method of face ends grinding of different diameters with turn of each next pusher 5 (Fig. 3a) by 180° is proposed. That equalizes the total normal cutting forces P_{nl} , P_{np} , the productivity of machining Q_l and Q_r (5) on the right p and the left l ends, wheels wearing I_{inl} , I_{inp} , the total technological systems flexibilities Y_{il} , Y_{ir} and increases the productivity and accuracy of grinding.

For the first time a model was developed that determines the torque from the cutting forces when grinding cylindrical circular parts of one and different diameters. The model describes the mechanism of the transition process occurrence at the input of the part in the machining area, stabilization of the process and the output of the part from the processing zone. With the help of this model one can perform an analysis of the accuracy of the part shape forming when leaving the machining area.

The 3D models are developed regarding the machining productivity of each face end of the part and the total productivity as well as the general method of theoretical and experimental research of the specific coordinates of processing on each face end, and the general: grinding productivity, power and cutting forces. This will promote the development of new ways of the face ends grinding and increase the efficiency of their evaluation.

References

1. Saturn. Tortcevoe shlifovanie sparennymi shlifoval'nymi krugami: [Zhurnal dlja klientov firmy «Junkermaschinen»]. Erwin Junker: Maschinenfabric Gmbh, Junkerstraße 2. Postfach 25. D 77787, Nordrash, Germany, 2005, 8 p. [In Russian].
2. Grabchenko A.I., Kalchenko V.I., Kalchenko V.V. Shlifovanie so skreshhivaiushchimisia osiami instrumenta i detail. Chernigov, ChDTU, 2009, 504 p. [In Russian].
3. Pat. Ukraine, No10636B24BMK15/04. Sposib odnochasnoho shlifuvannya dvokh tortsiv tsylindrychnykh detaley. V.V. Kal'chenko, O.V. Zhadan; zayavnyk ta patentovlasnyk: Kal'chenko V.V., Zhadan O.V. Nou200505125; Zayavl. 30.05.05; Publ. 15.11.05; Bull. No 11. [In Ukrainian].
4. Venzheha V.I. Pidvyshchennia efektyvnosti shlifuvannya tortsiv pry skhreshchenykh osiakh detali ta kruha z kalibruvalnoiu diliankoiu: diss... kand. tekhn. nauk:05.03.01, Venzheha Volodymyr Ivanovich; Kharkiv, National Technical University "Kharkiv Polytechnic Institute", 2009, 214p. [In Russian].
5. Kalchenko V.I., Venzheha V.I., Sliednikova O.S., Kalchenko D.V. Teoretychne ta eksperymentalne doslidzhennia protsesiv zniattia prypusku, znosu kruhiv, tochnosti formoutvorennya ta teplonapruzenosti pid chas shlifuvannya tortsiv detalei. Visnyk ChNTU. Seriya: Tekhnichni nauky, No.4 (6), 2016, pp. 25 – 34. [In Ukrainian].

6. Kalchenko V.I., Kalchenko V.V., Sliednikova O.S., Kalchenko D.V. Doslizhennia protsesu shlifuvania tortsiv orientovanykh detalei profilovanymy kruhamy. Visnyk ChSTU. Seriya: Tekhnichni nauky, No. 4, Cherkasy, 2016, pp. 72 – 82. [In Ukrainian].

Список використаної літератури

1. Saturn. Торцевое шлифование спаренными шлифовальными кругами: [Журнал для клиентов фирмы «Junkermaschinen»]. Erwin Junker: Maschinenfabric Gmbh, Junkerstraße 2. Postfach 25. D 77787. – Nordrath, Germany, 2005. – 8 с.
2. Грабченко, А.И. Шлифование со скрещивающимися осями инструмента и детали [Текст] / В.И. Кальченко, В.В. Кальченко – Издание 2-е, доп. Чернигов: ЧНТУ. – 2015. – 504 с.
3. Патент України № 10636В24ВМКл5/04. Спосіб одночасного шліфування двох торців циліндричних деталей [Текст] / Кальченко В.В., Жадан О.В.; заявники та патентовласники: Кальченко В.В., Жадан О.В. – № u200505125; заявл. 30.05.05; опубл. 15.11.05, Бюл. № 1.
4. Венжега, В.І. Підвищення ефективності шліфування торців при схрещених осях деталі та круга з калібрувальною ділянкою: дис... канд. техн. наук: 05.03.01 [Текст] / Венжега Володимир Іванович. – Харків, 2009. – 214с.
5. Кальченко, В.І. Теоретичне та експериментальне дослідження процесів знаття припуску, зносу кругів, точності формоутворення та теплонапруженості під час шліфування торців деталей [Текст]/В.І. Кальченко, В.І. Венжега, О.С. Следнікова, Д.В. Кальченко // Вісник Чернігівського національного технологічного університету. Серія: Технічні науки: науковий журнал. – Чернігів: ЧНТУ, 2016. – № 4 (6). – С. 25 – 34.
6. Кальченко, В.І. Дослідження процесу шліфування торців орієнтованих деталей профільованими кругами [Текст] / В.І. Кальченко, В.В. Кальченко, О.С. Следнікова, Д.В. Кальченко // Вісник Черкаського державного технологічного університету. Серія: Технічні науки. – Черкаси: ЧДТУ, 2016. – №4. – С. 72 – 82.

УДК 621.923

ТЕОРЕТИЧНЕ ТА ЕКСПЕРИМЕНТАЛЬНЕ ДОСЛІДЖЕННЯ ПРОЦЕСУ ДВОСТОРОННЬОГО ШЛІФУВАННЯ КРУГЛИХ ТОРЦІВ ОРІЄНТОВАНИМИ КРУГАМИ З КАЛІБРУЮЧИМИ ДІЛЯНКАМИ

Дмитро Кальченко

Чернігівський національний технологічний університет, Чернігів, Україна

Резюме. Розроблена 3D модель вперше визначає загальну продуктивність Q_s обробки двох круглих торців, наприклад, хрестовин, штовхачів, залежно від координати θ по всій дожині лінії контакту L . Вона дорівнює сумі продуктивностей шліфування всіх деталей, які знаходяться в зоні обробки на кожному з торців кругів. Вперше розроблена загальна методика теоретичного та експериментального досліджень питомих та загальних: продуктивності, потужності та сил різання на лівому та правому торцях деталі, сума яких дорівнює загальним продуктивностям на обох торцях. Розроблена методика визначення зв'язку поточної кутової координати осі деталі з необхідним часом обробки. Поки обробка деталі проводиться на калібруючій ділянці, наступна деталь не подається в зону обробки, що виключає вплив перехідного процесу на точність формоутворення, а продуктивність забезпечується за рахунок того, що наступна деталь входить у зону обробки одразу після виходу деталі з калібруючої ділянки.

Ключові слова: шліфування, торці деталей, орієнтовані шліфувальні круги, продуктивність шліфування.

Отримано 15.01.2018